

# LASER THIN GAS TARGET ACCELERATION FOR QUASI-MONOENERGETIC PROTON GENERATION

Min-Qing He<sup>#</sup>, Xi Shao, Chuan-Sheng Liu, Tung-Chang Liu, Jao-Jang Su, Galina Dudnikova, Roald Z. Sagdeev, East West Space Science Center, Department of Physics, University of Maryland, College Park, MD, USA  
 Zheng-Ming Sheng, Department of Physics, Shanghai Jiao Tong University, Shanghai, P.R.C and  
 Beijing National Laboratory for Condensed Matter Physics, Institute of Physics, CAS, Beijing, P.R.C.

## Abstract

We propose a scheme of laser thin gas target acceleration for quasi-monoenergetic proton generation. The scheme uses gas target of thickness about several laser wavelengths with gas density spatial distribution of Gaussian-like shape. We performed Particle-In-Cell simulation using circularly polarized laser of normalized maximum amplitude  $a = 1-5$  and hydrogen gas target of thickness 3-15 laser wavelength with peak density three times of the critical density. The simulation demonstrates several key physical processes involved in the laser thin gas target acceleration and the generation of quasi-monoenergetic protons. During the early phase of the laser plasma interaction, electron and ion cavities are observed. A compressed plasma layer is formed. The reflected protons in front of the compressed layer are accelerated and thus a bunch of quasi-monoenergetic protons are obtained. The compressed layer is finally destroyed due to Rayleigh-Taylor instability. The acceleration of the quasi-monoenergetic proton then stops with maximum energy about 5 MeV. It is also found that gas target thickness plays an important role for efficient quasi-monoenergetic proton generation.

## INTRODUCTIONS

Radiation pressure acceleration (RPA) has been considered as an efficient mechanism [1-3] for quasi-monoenergetic proton generation. Past work has been focused on the generation of quasi-monoenergetic protons through laser-thin solid target acceleration [1-7] and multi-MeV ion acceleration was achieved in experiment. Recently, there has been a great interest in both experiments and simulation of laser acceleration of hydrogen gas target for energetic proton generation [8]. The laser acceleration of gas targets is attractive since hydrogen gas is readily available and the laser can be of low-cost, long-duration and can deliver substantial amount of energy for proton acceleration.

Here, we present a scheme of laser thin gas target acceleration for quasi-monoenergetic proton generation. The scheme uses gas targets of thickness several laser wavelengths with the gas density spatial distribution being Gaussian or square sine shaped. For gas targets of

thin thickness ( $\sim$  several laser wavelength), the laser radiation pressure can compress the spatially-distributed proton gas into a thin layer of sub-wavelength thickness. The compressed thin layer of proton is over-dense and therefore can be accelerated by the laser radiation pressure in the same way as RPA until the development of the RTI destroys the opacity of the compressed layer. An example of RPA of a gas target from PIC simulation is shown below.

## SIMULATION PARAMETERS

Recent experiments showed that quasi-monoenergetic protons of several MeV was obtained from initially gaseous hydrogen target driven by an intense CO<sub>2</sub> laser. They found the acceleration is due to the shock generated by radiation-pressure driven hole boring of the critical surface [8]. In our paper, we present a set of particle-in-cell (PIC) simulations of laser thin gas target interactions with the incident laser of normalized amplitude  $a = eE_L/m_e c \omega = 1-5$  (i.e. laser intensities  $I = 10^{16}-10^{17} W/cm^2$ ),  $m_e$  is the electron mass,  $c$ ,  $\omega$  and  $E_L$  are the light speed in vacuum, the laser frequency and electric field, respectively. The incident circularly polarized laser is a plane wave in transverse direction and the time profile of its amplitude is  $a = a_0 \sin^2(t\pi/T_r)$ , where the rise time  $T_r = 150$  laser period. The PIC simulation domain is within  $0 \leq x/\lambda_L \leq 30$ ;  $0 \leq y/\lambda_L \leq 10$ . The gaseous plasma is initially located at  $6 \leq x/\lambda_L \leq 11$  with initial spatial plasma density profile being  $n_0 \sin^2[(x/\lambda_L - 6) \pi/l_s]$ , where target thickness  $l_s$  has been varied from 5 to 15  $\lambda_L$  with  $\lambda_L = 10 \mu m$  being the laser wavelength, and peak target density  $n_0$  is varied from  $n_c$  to  $20 n_c$ , where  $n_c \approx 1.1 \times 10^{19} cm^{-3}$  is the critical density.

## CAVITON FORMATION AND ION ACCELERATION

As the laser is incident on the gas target, it is reflected at where the gas target density matches the critical density. At this reflection point, the ponderomotive force pushes the electrons on the right forward and those on the left backward, creating a local electron density dip. This density dip further traps the laser radiation within the dip and the ponderomotive pressure of the incident and reflected laser further depletes electrons in the trap,

<sup>#</sup>minqinghe@gmail.com

producing an electron cavity, see Fig. 1 (a). The high electron density peaks formed on the two sides of the electron cavity pull ions in both directions with electrostatic force over the ion motion time scale and two local ion density peaks are produced around the electron cavity, leading to the formation of ion cavity as well. So a plasma vacuum is formed near the location of critical density. Because the ions and electrons are not overlap completely at the cavity edge, a positive electrical static field along the laser propagation direction is formed, see Fig. 1 (b). This electric field can accelerate the protons in the front.

The plasma on the front side is continuously compressed by the laser radiation with increasing intensity and the relativistic increase of electron mass leads to the penetration of the laser into the high density regions over the plasma skin depth. The laser with increasing intensity compresses the plasma front, leading to the formation of a layer of electron density increased to 10 times critical density for the case with  $a_0=2$ ,  $l_s=5$ ,  $n_0=3n_c$ , see Fig. 1 (d) and (e). The peak density steepens [9-10] and its front moves forward and creates upstream electron oscillation. Some of the electrons are accelerated to the rear ends of the plasma.

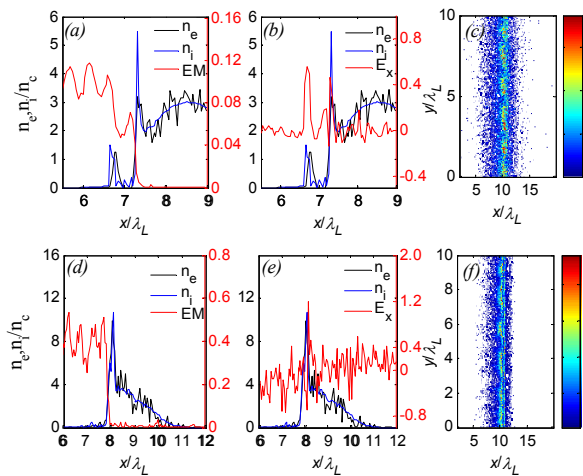


Figure 1: 2D PIC simulation results of parameters  $a_0=2$ ,  $l_s=5$ ,  $n_0=3n_c$  (a) and (d) are electron, ion density and laser electric and magnetic energy density plot at  $t=70 T_L$  and  $t=110 T_L$ , respectively; (b) and (e) are electron, ion density and electric field plot at  $t=70 T_L$  and  $t=110 T_L$ , respectively; (c) and (f) are electron and ion density (normalized by  $n_c$ ) map at  $t=170 T_L$ , respectively.

The thickness  $\Delta_s$  of compressed high density plasma layer is less than  $l\lambda_L$ . Within this thin layer, electron layer is pushed by the laser radiation pressure and proton layer is accelerated by electrostatic force from the electron layer. Together they form a self organized double layer.

Protons trapped within the double layer can be accelerated to 1 MeV and maintain quasi-monoenergetic property, see Fig. 2. From the ion energy phase space

plots in Fig. 2, we observed four acceleration mechanisms in our simulation:

- at the plasma rear side, target normal sheath acceleration (TNSA) due to the electric field from the hot electrons exiting the plasma.
- Brillouin back scattering on the front side.
- Shock-like acceleration due to the ion-reflection at the front of the compressed layer in the plasma [9-12].
- Radiation pressure acceleration pushes the compressed double layer to obtain the quasi-monoenergetic ion bunch.

The dominant acceleration mechanism for quasi-monoenergetic proton generation is the radiation pressure acceleration developed at later stage. The compressed thin double layer becomes unstable due to the R-T instability. Density blobs are formed (see Fig. 1 (c) and (f)) and the laser light starts to leak out of the under-dense region created by the R-T instability. The quasi-monoenergetic property of the proton beam is finally destroyed due to the R-T instability.

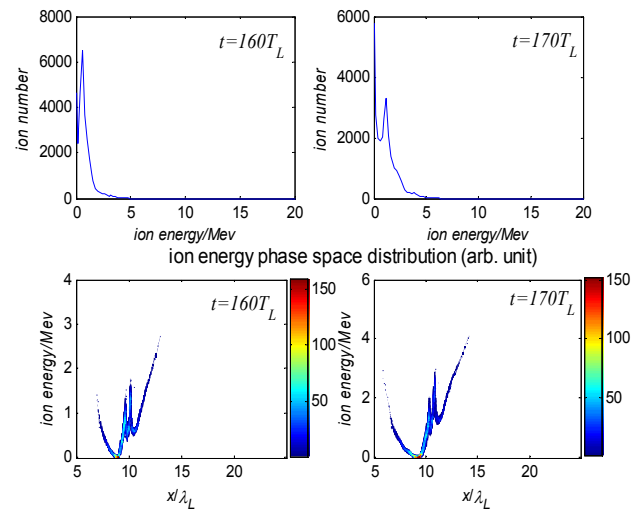


Figure 2: 2D PIC simulation results of energy spectrum (the first row) and ion energy phase space distribution (the second row) at  $t=160 T_L$  and  $t=170 T_L$  for simulation with parameters  $a_0=2$ ,  $l_s=5$ ,  $n_0=3n_c$ .

To further investigate the caviton formation and ion acceleration, we changed the laser and plasma parameters in our simulation: laser intensity  $a_0$  from 1 to 10,  $l_s$  from 3 to  $15\lambda_L$ , and  $n_0$  from 1 to  $20 n_c$ . We found that if we increased the target thickness  $l_s$ , more cavitons are formed. The plasma with wider spatial distribution gives enough space to form multi-cavitons.

Increasing  $a_0$  and  $n_0$ , we can get higher quasi-monoenergetic spectrum. If we use simulation parameters  $a_0=5$ ,  $l_s=5$ ,  $n_0=10n_c$ , we can get the ion energy up to 5 MeV (figure 3). The RT instability evolves slowly and the compressed layer is destroyed later in figure 3 than the case with simulation parameters  $a_0=5$ ,  $l_s=5$ ,  $n_0=3n_c$  as shown in Fig. 2.

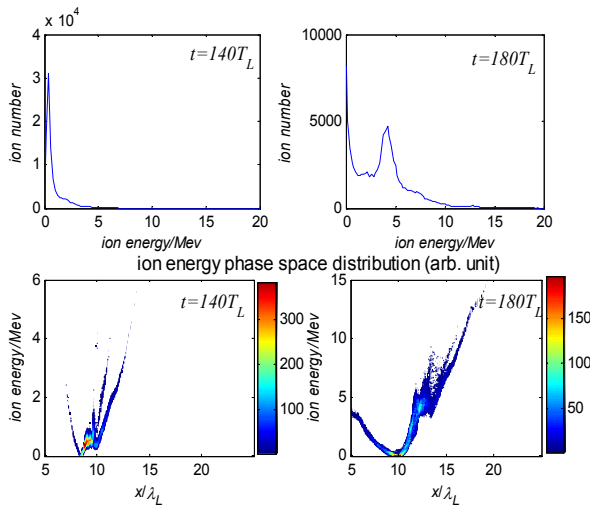


Figure 3: 2D PIC simulation results of energy spectrum (the first row) and ion energy phase space distribution (the second row) at  $t=140 T_L$  and  $t=180 T_L$  for simulation with parameters  $a_0=5$ ,  $l_s=5$ ,  $n_0=10n_c$ .

### CONCLUSIONS

Laser gas thin target interaction is a promising mechanism in generation of quasi-monoenergetic protons. Caviton formation can assist the creation of the compressed ion layer. Decreasing the thickness of the plasma, increasing the laser intensity and plasma density can help to obtain higher energy quasi-monoenergetic ions.

### REFERENCES

- [1] X. Q. Yan et al., Phys. Rev. Lett. 100,135003(2008).
- [2] B. Qiao et al. Phys. Rev. Lett. 102, 145002(2009).
- [3] C. S. Liu, X. Shao, B. Eliasson, T. C. Liu, G. Dudnikova, R. Z. Sagdeev, AIP Conf. Proc. 1320, 104 (2011).
- [4] T. C. Liu et al., submitted.
- [5] A. Macchi et al., Phys. Rev. Lett. 94,165003(2005).
- [6] B. M. Hegelich et al., Nature(London) 439,441(2006). H. Schworer et al., Nature(London) 439, 445(2006).
- [7] A. P. L. Robinson et al., New J. Phys. **10** 013021(2008).
- [8] C. A. J. Palmer, N. P. Dover, I. Pogorelsky, M. Babzien, G. I. Dudnikova, M. Ispiriyan, M. N. Polyanskiy, J. Schreiber, P. Shkolnikov, V. Yakimenko, and Z. Najmudin, Phys. Rev. Lett. 106, 014801(2011).
- [9] S. C. Wilks et al., Phys. Rev. Lett. 69, 1383(1992).
- [10] M. Q. He, Q. L. Dong, Z. M. Sheng, S. M. Weng, M. Chen, H. C. Wu, and J. Zhang, Phys. Rev. E, 76,035402(R)(2007).
- [11] M. Q. He, Q. L. Dong, Z. M. Sheng, S. M. Weng, M. Chen, H. C. Wu, and J. Zhang, Acta Phys. Sinica,58,363(2009)(in Chinese).
- [12] M. Q. He, Q. L. Dong, Z. M. Sheng, S. M. Weng, M. Chen, H. C. Wu, and J. Zhang, Journal of Physics, 112,042046 (2008).